Identification of reconstruction in Pt films deposited on Pd(110) at room temperature

P. J. Schmitz,* W.-Y. Leung, H. C. Kang,† and P. A. Thiel
Department of Chemistry and Ames Laboratory, Iowa State University, Ames, Iowa 50011
(Received 14 February 1991; revised manuscript received 24 June 1991)

We have studied the properties of Pt films on Pd(110), grown by deposition at 300 K and annealed up to 900 K, using low-energy electron diffraction and Auger-electron spectroscopy. We observe (1×2) and (1×3) superstructures, depending upon Pt coverage and annealing temperature. At one monolayer, the (1×1) periodicity is unperturbed. Between one and three monolayers, a broad and streaky (1×2) develops upon annealing, then fades to (1×1) as the film dissolves. At three monolayers and above, the broad and streaky (1×2) splits to a (1×3), then fades again to (1×1) at high temperature. Adsorption of CO causes $(1\times3)\rightarrow(1\times1)$ reversion at relatively low temperature, 430 K. Based upon the known behavior of Pt(110) reconstructions, this is strong evidence that the (1×3) structure of the Pt film is a surface reconstruction.

I. INTRODUCTION

Properties of thin films, including surface properties, are being scrutinized ever more closely. One intriguing, fundamental property of a surface is its tendency to undergo a structural transformation, or reconstruction, wherein the surface atoms are displaced from their bulklike positions, with a component of that displacement in the surface plane.[1] While there is a large body of literature concerning reconstructions in clean surfaces of *bulk* materials, as yet there are very few studies of surface reconstruction of *films*. In this paper, we describe such a study for one particular metal film system, Pt/Pd.

Pt and Pd are very similar metals. The lattice mismatch, for instance, is only 0.8% (Ref. 2) and so lattice strain should present little perturbation to the surface properties when one metal is grown atop another. The two metals also are continuously miscible in the solid state.[3] However, a major difference in their properties is that the clean, low-index surfaces of bulk Pt tend to reconstruct, whereas the clean, low-index surfaces of bulk Pd are stable against reconstruction.[4,5] Specifically, for the clean (110) surface of Pt, as well as Au and Ir, $(1\times n)$ "missing-row" reconstructions are known, where n can take values of 2, 3, and even higher integers.[1] For clean Pt(110), the (1×2) reconstructions are most frequently reported in the literature[6–22] but (1×3) structures have also been described.[6–9]

In this study we show that Pt films grown on the (110) surface of Pd can exhibit bulklike reconstruction. The two parameters which we vary in searching for reconstruction are coverage and annealing temperature. Coverage is important because it indicates the thickness at which this particular surface property—reconstruction—approaches that of the bulk. Temperature is important because the $(1\times1)\rightarrow(1\times2)$ transformation of the bulk (110) surface is an activated and irreversible process, known to require temperatures of 275–300 K to occur on typical experimental time scales.[12] This reflects the energy barrier associated with surface diffusion in forming the missing-row reconstruction,[13] and so it is reasonable that thermal treatment is also necessary to induce reconstruction in the Pt film. There are no previous studies of Pt/Pd(110) reported in the literature.

II. EXPERIMENTAL PROCEDURES

The experiments take place in an ultrahigh vacuum system equipped for Auger-electron spectroscopy (AES), mass spectrometry, ion bombardment, low-energy electron diffraction (LEED), and Pt evaporation. The Pt source is a resistively heated tungsten filament wrapped with 0.25-mm-diam Pt wire (99.95%), following the design of DeCooman and Vook.[23] The Pt source is enclosed in a double-walled, liquid-nitrogen-cooled shroud with a 1.5-cm orifice directed toward the sample. The deposition rate is on the order of 10^{13} atoms s^{-1}. Using a thoroughly outgassed filament, 60 s of evaporation usually causes the pressure to rise by $\sim4\times10^{-10}$ Torr above background, which is $\leq2\times10^{-10}$ Torr. AES reveals no impurities in the films, and shows that the distribution of Pt across the sample is uniform within $\pm5\%$. The Pt is removed by argon-ion bombardment after each experiment. The conditions of bombardment are 1 keV, approximately 1.5 $\mu A/cm^2$, at 300 K.

In the annealing sequences, the crystal is held for 20 s at temperature, then cooled below 200 K for LEED and AES measurements. Therefore, only *irreversible* changes are detected. The diffraction pattern is recorded via a silicon-intensified-target camera on a videotape, and later processed with a computerized image-acquisition system.[24] The LEED intensity profiles are measured along the [001] direction, i.e., between the reciprocal-space (1,0) and (1,1) positions. Diffuse intensity elongated between these two reciprocal-space positions is referred to as streaking. The crystal current is 70 nA. More experimental details can be found elsewhere.[25,26]

III. EXPERIMENTAL RESULTS

Coverage determination. For estimation of Pt film thickness, we use mainly AES. Figure 1 displays the $Pt_{64}(NVV)$ and $Pd_{330}(MNN)$ signal intensities as a function of cumulative deposition time at 300 K. As in a previous study of Pt/Pd(100),[27] there are no clear discontinuities in slope to indicate the filling of successive layers; however, the absence of such discontinuities does not rule out layer-by-layer growth.[27] We therefore estimate the Pt to Pd Auger ratios expected at $\Theta_{Pt}=1$ and 2.[28] [The absolute coverage is expressed in monolayers Θ, and is defined as the ratio of surface atoms to atoms in a bulk Pd(110) plane, 9.35×10^{14} cm^{-2}.] Using inelastic mean free paths for the $Pd_{330}(MNN)$ and $Pt_{64}(NVV)$ Auger electrons of 7 and 4 Å, respectively,[29,30] and handbook spectra for a measure of the peak-to-peak intensity of bulk Pt relative to Pd,[31] the calculated Auger intensity ratio (I_{Pt}/I_{Pd}) is 0.34 and 0.71 at $\Theta=1$ and 2, respectively. These ratios (0.30–0.35 and 0.7–0.8) are indicated with arrows in Fig. 1. Their assignment to coverages of 1 and 2, respectively, is substantiated by a previous study of Pt on Pd(100), wherein layer growth and coverages were established somewhat more reliably using Bragg intensity oscillations in LEED.[32] The values obtained for the Auger ratio of Pt to Pd in that work were 0.30 for the first layer and 0.77 for the second layer.[32] We therefore take the arrows in Fig. 1 to indicate, at least roughly, the points where the first and second layers are filled. It takes about twice as long to reach the second value as the first, indicating that the film grows in a somewhat smooth (layered) morphology, at least for the first two layers and at 300 K. Higher experimental AES ratios are assigned to integral coverages by assuming that Pt flux and sticking coefficient are invariant with time. The assumption of constant sticking coefficient is supported by our previous studies of Pd/Pd(100) and Pt/Pd(100).[32,33] Nonetheless, at $\Theta_{Pt}>2$, the values should only be taken to indicate relative, not absolute, coverages.

Film superstructures. Figure 2 shows the LEED intensity profiles for a series of Pt films as a function of annealing temperature following deposition at 300 K, and Table I summarizes the results. At $\Theta_{Pt}=1$, the (1×1) periodicity appears unperturbed, and no fractional order spots or streaking are visible. As Θ_{Pt} increases to 2, heavy streaking appears. At $\Theta_{Pt}=2$, some intensity grows at the half-order position after annealing to 370–400 K, as shown in Fig. 2(a). This fractional-order intensity is very broad, and disappears after annealing to temperatures greater than 575 K. At $\Theta_{Pt}=3$, Fig. 2(b), the same streaking appears but as the temperature increases to 550 K the half-order spot intensifies and sharpens slightly; at higher temperature the half-order spot splits and moves, reaching third-order positions at 630 K. Annealing to higher temperature results in complete loss of the fractional-order components.

The continuous splitting of the half-order spot with increasing temperature, resulting finally in a (1×3) super-

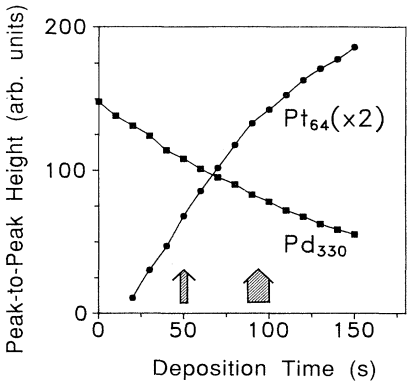

FIG. 1. Pt and Pd Auger intensities as a function of cumulative Pt deposition time at 300 K. The Auger data are acquired in the first-derivative mode with a single-pass, cylindrical mirror analyzer and a normal-incidence electron gun (2 keV).

TABLE I. Temperature- and coverage-dependent progression of LEED patterns, following deposition of Pt on Pd(110) at 300 K.

Coverage	Structural sequence with increasing temperature
$\Theta_{Pt}=1$	(1×1)
$\Theta_{Pt}=2$	streaky (1×1) $\xrightarrow{400\ K^a}$ broad (1×2) $\xrightarrow{575\ K}$ (1×1)
$\Theta_{Pt}=3$	streaky (1×1) $\xrightarrow{400\ K^a}$ broad (1×2) $\xrightarrow{575-630\ K^b}$ (1×3) $\longrightarrow$ (1×1)
$\Theta_{Pt}=5$	streaky (1×1) $\xrightarrow{400\ K^a}$ broad (1×2) $\xrightarrow{460-760\ K^b}$ (1×3) $\xrightarrow{785K}$ (1×1)
$\Theta_{Pt}=15$	streaks $\xrightarrow{490\ K^a}$ broad (1×2) $\xrightarrow{710-885\ K^b}$ (1×3) $\longrightarrow$ (1×1)

[a]The distinction between a streaky (1×1) (or streaks alone) and a broad (1×2) is rather subjective, as Fig. 2 reveals. Therefore the temperature at which the transition between these two patterns occurs is also subjective.

[b]In these temperature regimes, the LEED pattern changes continuously from a relatively broad and faint (1×2), to a sharper and brighter (1×3).

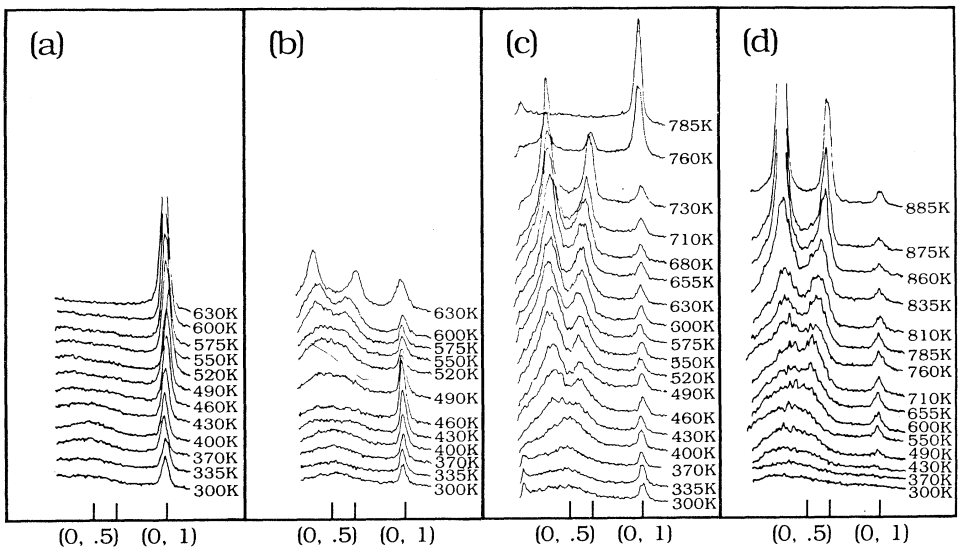

FIG. 2. LEED profiles measured along the [001] direction between the (0,0) and (0,1) beams at a beam energy of 35 eV. The approximate Pt coverages are (a) $\Theta=2$, (b) $\Theta=3$, (c) $\Theta=5$, (d) $\Theta=15$.

structure, is more apparent for thicker Pt films as evident in Figs. 2(c) and 2(d). At $\Theta_{Pt}=5$, Fig. 2(c), a broad half-order spot appears after heating to 400 K, which splits and shifts continuously as the temperature increases further. Annealing to 760 K produces a bright (1×3) pattern. Higher temperatures result in loss of the (1×3) and return of the (1×1). At $\Theta_{Pt}=15$, Fig. 2(d), the broad half-order spot persists to 710 K, splits at higher temperature, and reaches third-order positions at 885 K. The (1×1) returns at higher temperature.

The temperature necessary to gain (1×3) periodicity increases as coverage increases. This is illustrated in Fig. 3, whereas $\Delta k_{\parallel}$ of the component which develops into the $(0,\frac{2}{3})$ spot is shown as a function of temperature for three Pt coverages. The temperature necessary to reach $\Delta k_{\parallel}=\frac{1}{3}$ is 630, 760, and 885 K for $\Theta_{Pt}=3$, 5, and 15, respectively. For each coverage, this coincides with the temperature at which the fractional-order spots reach maximum intensity prior to fading. Note also that the maximum intensity of the fractional-order pattern increases as coverage increases. That is, the brightest (1×3) of Fig. 2(d) is 1.5 times more intense than that of Fig. 2(c), and it is 3 times more intense than that of Fig. 2(b).

Auger measurements: thermal stability of films. The variation of the I_{Pt}/I_{Pd} Auger ratio with temperature is shown in Fig. 2. Note that the temperature programs and coverages are identical to those of Fig. 2, except for the highest coverage, which is $\Theta_{Pt}=15$ in Fig. 2 and $\Theta_{Pt}=10$ in Fig. 4. The reason for the difference is that an

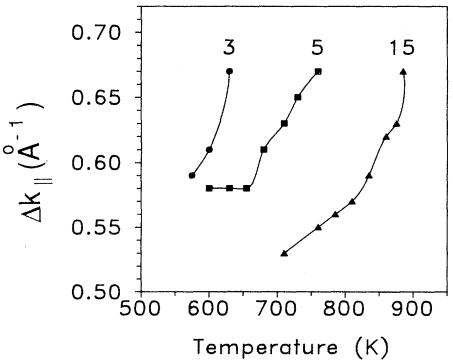

FIG. 3. LEED spot splitting as a function of temperature for three initial coverages of Pt. Each curve is labeled with the initial Pt coverage in monolayers.

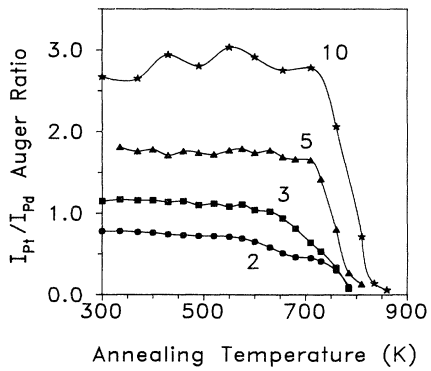

FIG. 4. I_{Pt}/I_{Pd} Auger ratio as a function of annealing temperature. Each curve is labeled with the initial Pt coverage in monolayers. The ten-monolayer curve is compressed vertically by a factor of 10, and the five-monolayer curve by a factor of 2.

Auger ratio cannot be measured meaningfully for Pt films thicker than $\Theta_{Pt}=10$. With this exception, the Auger data of Fig. 4 are exactly comparable to the LEED data of Fig. 2 and, in fact, are acquired simultaneously.

It is evident that the I_{Pt}/I_{Pd} Auger ratio declines as temperature increases. For $\Theta_{Pt}=2$ and 3, the most severe decline begins approximately at 600 K; for $\Theta_{Pt}=5$ and 10, the decline begins at 700 K. [The former temperature is about 100 K lower than that reported in a similar study of Pt on Pd(100), for comparable Pt coverages.[27]] Comparison of the AES and LEED data reveal that the (1×3) disappears, and the (1×1) returns, only after a significant diminution of the Pt Auger signal at all coverages. This might be expected, since both events probably signal massive dissolution of Pt in Pd. More unexpected is the correlation between the fractional-order spots' sharpening and splitting toward third-order positions, and the decline in the Auger ratio. Although this correlation is ambiguous for the two lower coverages, where the Auger ratio declines gradually, it is evident for the two higher coverages, where the Auger ratio is constant and then falls off sharply. For instance, when a five-layer film is annealed at 760 K, the Auger ratio falls to 75% of its original value (cf. Fig. 4), yet here the fractional-order LEED spots reach third-order positions and become much brighter than at any other temperature [cf. Fig. 2(c)]. The (1×3) then fades and disappears at $T>760$ K [cf. Fig. 2(c)].

Adsorption of CO. It is known that adsorption of certain gases, particularly CO, can cause the (1×2) and (1×3) patterns of *bulk* Pt(110) to revert to the (1×1).[7,20,19,6,21,22] Therefore we examine the effect of CO adsorption on the (1×3) superstructure of the Pt film, in order to determine if the film behaves similarly. Adsorption of CO at temperatures below 400 K does not remove the (1×3) pattern of the film; exposure at higher temperature (430 K) *does* lift the (1×3), as shown in Fig. 5. This indicates that the CO-induced (1×3)→(1×1) reversion is activated. Working at $T>400$ K introduces a complication, however, in that the desorption rate of CO is significant and a CO adlayer is not stable in vacuum. In order to establish an equilibrium coverage of CO at this temperature, the LEED measurements are performed in ambient CO (1×10^{-8} Torr). Figure 5 shows that the (1×3) is removed slowly under these conditions. It is not clear whether the time dependence results from a slow increase in CO coverage, from the kinetics of the (1×3)→(1×1) transition, or from both (perhaps coupled). In any case, the (1×3) is removed with CO adsorption at 430 K, as shown, and it also returns when CO desorbs (not shown).

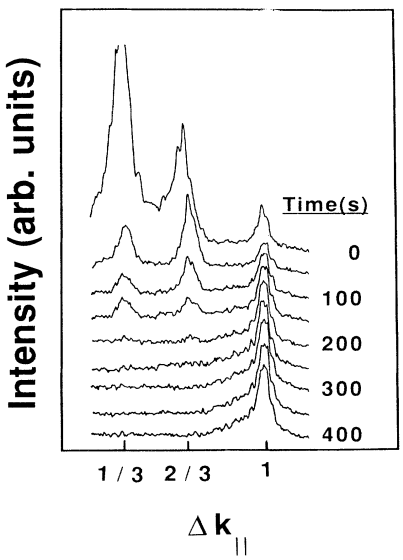

FIG. 5. LEED profiles acquired during continuous exposure of a Pt film ($\Theta_{Pt}=3$) to CO at 430 K. The pressure of CO is 1×10^{-8} Torr. The film is initially prepared by deposition of Pt at 300 K in vacuum, followed by annealing to 630 K. The annealing produces a (1×3) with optimal brightness and sharpness at this coverage (cf. Fig. 2).

IV. DISCUSSION

A first main conclusion from the data is that the Pt films exhibit LEED patterns with (1×2) and (1×3) periodicity. The same periodicity is associated with the known missing-row reconstructions of Pt(110), suggesting strongly that they share a common origin. However, the Auger ratio of the film (Fig. 4) declines significantly before the "best" (1×3) is obtained (Fig. 2). This could be interpreted as evidence that the (1×3) represents an *ordered surface alloy* rather than a surface reconstruction. We believe that this interpretation is incorrect, based on the fact that the (1×2) and (1×3) superstructures first appear when there is no appreciable change in the Auger ratio. As shown in Fig. 2, the broad spots of the (1×2) appear at 300 K, whereas the (1×3) pattern appears at higher temperatures: 575 K at $\Theta=3$, 460 K at $\Theta=5$, and 710 K at $\Theta=15$. If these structures were due to different surface alloys, the Auger ratio should be constant at all coverages for the (1×2) or (1×3) patterns, and should change when (1×2) converts to (1×3). However, no such correlation is observed. On the other hand, the decline in the Auger ratio of the film for the best (1×3) suggests that partial dissolution of the Pt film accompanies some change in morphology. In addition, the adsorption of CO (Fig. 5) causes the LEED pattern to change from (1×3) to (1×1). This is very similar to the effect of CO adsorption on the Pt(110) surface, where it is known that CO can "lift" the reconstruction.[6,7,19–22] If the (1×3) pattern of the Pt film represented a Pt-Pd alloy, it is unlikely that adsorption of CO could cause reversion to (1×1). Therefore we classify the (1×3) pattern of a film as a missing-row reconstruction, analogous to those identified for bulk Pt(110) surfaces.[7,9–11,13–17,19] The temperature necessary for this process to occur with the film—430 K—is comparable to the temperature necessary for CO to lift the known (1×3) reconstruction of Pt(110)—300 to 400 K.[7]

For the Pt film, deposition at 300 K results in a streaky (1×1) pattern. The streaks surely indicate that some de-

gree of (1×2) order is present, although the deposition process must "trap" a high degree of disorder. A recognizable (1×2) LEED pattern is obtained after annealing to 400–500 K. This temperature range is significantly higher than that reported for clean (110) surfaces of bulk Pt, where the (1×1)→(1×2) transition reportedly occurs at 275–300 K, depending upon heating rate.[12] Because of the long annealing times in our experiments, the value which corresponds to the slowest heating rate (275 K) is most appropriate for comparison to our data. Thus the kinetics of the (1×1)→(1×2) transition are somewhat slower for the film than for the bulk surface, perhaps due to roughness in the film which inhibits diffusion.

At $\Theta_{Pt} \geq 3$, the LEED pattern changes continuously from (1×2) to (1×3) with increasing temperature, as shown by Fig. 2 and Table I. At lower coverage, the full progression to the (1×3) does not occur; we postulate that it is prevented by extensive Pt-Pd mixing at relatively low temperature. Indeed, the Auger data of Fig. 4 show that at $\Theta_{Pt} < 3$ the films are less stable than at higher coverage. For $\Theta_{Pt} \geq 3$, the (1×2) predominates after low-temperature annealing (approximately 400–500 K); the (1×3) predominates after high-temperature annealing (approximately 600–900 K); and in between, the surface contains a mixture of (1×2) and (1×3) domains. In the mixed regime, the (1×2) and (1×3) domains must be small relative to the coherence length of the LEED optics (approximately 100 Å) in order to explain the continuous shift in spot position. The smallness of the (1×2) domains is also obvious from the broadness of the $(0, \frac{1}{2})$ spot after low-temperature annealing (cf. Fig. 2). The half-width corresponds to a real-space dimension of 10 to 13 Å, or 4 to 5 unit cells. By contrast, the third-order spots of the (1×3) structure are much sharper, particularly for the thicker films, where their width approximately equals that of the (0,1) spot. It appears that small regions of (1×2) develop at 400–500 K, but then (1×3) regions also develop at higher temperature and eventually engulf the (1×2) areas. This suggests that formation of the (1×3) is slower than formation of the (1×2) at low temperature—possibly reflecting a higher activation barrier—but that the (1×3) is more stable than the (1×2).

It is interesting that the (1×3) structure is favored for thick Pt films, even though the (1×2) structure is most often reported for (110) surfaces of bulk Pt.[6–22] It is, in fact, remarkable that the sharpest and brightest (1×3) pattern is observed for the thickest film [$\Theta_{Pt} = 15$, Fig. 2(d)], since one would expect a thick film to approach bulklike properties. Some unique characteristic of the film must favor the (1×3) structure over the (1×2). There are two obvious possibilities. The first is that the Pt film changes in morphology—either roughens or smoothens—as temperature increases, and this change in morphology favors the (1×3). This hypothesis is supported by results for Au/Pd(110), where the (1×3) reconstruction appears to be associated with thicker films because of the roughness which is introduced to the film above a critical coverage.[34] For Pt/Pd(110), neither Auger nor LEED data provide unequivocal evidence for a temperature-dependent morphological change, although the slight decline in the Auger ratio at $T < 600$ K and $\Theta_{Pt} < 5$ (Fig. 4) could be taken as evidence of roughening. The second hypothesis is that the (1×3) is stabilized by small amounts of Pd impurities in the Pt film, and that annealing serves to increase the surface concentration of such impurities, even before AES clearly reveals such intermetallic mixing. Indeed, other authors have shown that the (1×2) reconstruction of Pt(110) can be converted to the (1×3) phase by trace amounts of Ca and K, which can be explained by the propensity for electron transfer from these contaminants to the metal.[8,9,35,36] (Neither Ca nor K is detectable with AES as an impurity in our Pt films or Pd substrate.) If some electron transfer occurred also from Pd to Pt, this might explain the stabilization of the (1×3). If the boundary between Pt and Pd were perfectly sharp, such an effect should be limited to the region close to the interface. However, the slight decline in the Auger ratio at $T < 600$ K and $\Theta_{Pt} < 5$ (Fig. 4) could be taken as evidence of gradual intermixing of the two metals, with the sensitivity to such intermixing being lower for the thicker films. Thus both hypotheses are plausible, on the basis of data presently available.

Finally, it is interesting to note that Au films grown on Pd(110) also display a continuous progression from (1×2) to (1×3) LEED patterns.[26,34] However, there are two major differences between the two systems. First, in the case of Au/Pd(110) the fractional-order spot splitting is primarily a function of coverage, not annealing temperature, whereas the reverse is true of Pt/Pd(110). A second major difference is that, although the Au/Pd(110) LEED pattern attains third-order periodicity at $\Theta_{Au} \approx 4$, the pattern becomes increasingly faint above two monolayers, and disappears entirely above approximately six monolayers. In contrast, the (1×3) pattern of Pt/Pd(110) gets brighter and brighter with coverage, at least up to 15 monolayers. In the case of Au/Pd(110), we attribute the LEED patterns to the growth mode of the film, which is Stranski-Krastanov with a critical thickness of two monolayers.[26,34] Further experimental data, such as scanning tunneling microscopy, are necessary to determine whether the (1×2) and (1×3) patterns of Pt/Pd(110) can be similarly associated with coverage- or temperature-dependent changes in gross morphology.

V. CONCLUSIONS

There are two main results from this study.

(1) Annealing Pt films can produce LEED patterns with (1×2) and (1×3) periodicity, at Pt coverages above two monolayers. The fact that CO adsorption lifts the (1×3) is evidence that the pattern represents a bulklike, missing-row reconstruction.

(2) The temperature-dependent progression of the LEED patterns suggests that small (1×2) domains develop first, at relatively low temperature. The (1×3) domains form and grow at higher temperature, eventually overwhelming the (1×2) areas. Some property of the film—perhaps roughness or a small amount of Pt-Pd mixing—serves to favor the (1×3) over the (1×2) struc-

ture. At even higher temperature, the LEED pattern fades to a (1×1), probably due to massive dissolution.

ACKNOWLEDGMENTS

We thank R. J. Baird and G. W. Graham of Ford Motor Company for the use of their Pd(110) crystal, and J. W. Rabalais for providing Refs. 8 and 10 prior to publication. This work was initiated under National Science Foundation Grant No. CHE-8451317 (for P.A.T.) and continues under Materials Chemistry Initiative Grant No. CHE-9014214. It is also supported by the Camille and Henry Dreyfus Foundation (P.A.T.) and by the Ford Motor Company. One of us (P.J.S.) acknowledges partial support by Phillips Petroleum. In addition, some equipment and all facilities are provided by the Ames Laboratory, which is operated for the U.S. Department of Energy by Iowa State University under Contract No. W-7405-ENG-82.

*Present address: Ford Motor Company, Dearborn, Michigan 48121.

†Present address: Department of Chemistry, National University of Singapore, Singapore.

[1]P. J. Estrup, *Chemistry and Physics of Solid Surfaces V,* edited by R. Vanselow and R. Howe (Springer, Berlin, 1984), p. 205.

[2]C. Kittel, *Introduction to Solid State Physics,* 5th ed. (Wiley, New York, 1976), p. 31.

[3]M. Hansen, *Constitution of Binary Alloys* (McGraw-Hill, New York, 1958), p. 1121.

[4]M. Wolf, A. Goschnick, J. Loboda-Cackovic, M. Grunze, W. N. Unertl, and J. H. Block, Surf. Sci. **182**, 489 (1987).

[5]R. D. Diehl, M. Lindroos, A. Kearsley, C. J. Barnes, and D. A. King, J. Phys. C **18**, 4069 (1985).

[6]M. Salmeron and G. A. Somorjai, Surf. Sci. **91**, 373 (1980).

[7]P. Fery, W. Moritz, and D. Wolf, Phys. Rev. B **38**, 7275 (1988).

[8]F. Masson and J.W. Rabalais (unpublished).

[9]M. Stock, J. Risse, U. Korte, and G. Meyer-Emsen, Surf. Sci. **233**, L243 (1990).

[10]F. Masson and J. W. Rabalais (unpublished).

[11]P. Fenter and T. Gustafsson, Phys. Rev. B **38**, 10 197 (1988).

[12]S. Ferrer and H. P. Bonzel, Surf. Sci. **119**, 234 (1982).

[13]G. L. Kellogg, Phys. Rev. Lett. **55**, 2168 (1985).

[14]Q. Gao and T. T. Tsong, Phys. Rev. Lett. **57**, 452 (1986).

[15]E. Vlieg, I. K. Robinson, and K. Kern, Surf. Sci. **233**, 248 (1990).

[16]E. C. Sowa, M. A. Van Hove, and D. L. Adams, Surf. Sci **199**, 174 (1988).

[17]H. Niehus, Surf. Sci. **145**, 407 (1984).

[18]D. L. Adams, H. B. Nielsen, M. A. Van Hove, and A. Ignatiev, Surf. Sci. **104**, 47 (1981).

[19]T. E. Jackman, J. A. Davies, D. P. Jackson, W. N. Unertl, and P. R. Norton, Surf. Sci. **120**, 389 (1982).

[20]T. Gritsch, D. Coulman, R. J. Behm, and G. Ertl, Phys. Rev. Lett. **63**, 1086 (1989).

[21]R. Imbihl, S. Ladas, and G. Ertl, Surf. Sci. **206**, L903 (1988).

[22]C. M. Comrie and R. M. Lambert, J. Chem. Soc. Faraday Trans. 1 **72**, 1659 (1976).

[23]B. C. DeCooman and R. W. Vook, J. Vac. Sci. Technol. A **21**, 899 (1982).

[24]J. W. Anderegg and P. A. Thiel, J. Vac. Sci. Technol. A **4**, 1367 (1986).

[25]P. J. Schmitz, Ph.D. thesis, Iowa State University, 1990.

[26]P. J. Schmitz, H. C. Kang, W.-Y. Leung, and P. A. Thiel, Surf. Sci. (to be published).

[27]S. L. Beauvais, R. J. Behm, S.-L. Chang, T. S. King, C. G. Olson, P. R. Rape, and P. A. Thiel, Surf. Sci. **189/190**, 1069 (1987).

[28]S. H. Lu, J. Quinn, D. Tian, and F. Jona, Surf. Sci. **209**, 364 (1989).

[29]S. Xinyin, D. J. Frankel, J. C. Hermanson, G. J. Lapeyre, and R. J. Smith, Phys. Rev. B **32**, 2120 (1985).

[30]P. W. Palmberg, Anal. Chem. **45**, 549A (1973).

[31]P.W. Palmberg, G. E. Riach, R. E. Weber, and N. C. MacDonald, *Handbook of Auger Electron Spectroscopy* (Physical Electronics Industries, Edina, MN, 1972).

[32]D. K. Flynn, W.-D. Wang, S.-L. Chang, M. C. Tringides, and P. A. Thiel, Langmuir **4**, 1096 (1988).

[33]D. K. Flynn, Ph.D. thesis, Iowa State University, 1990.

[34]P. J. Schmitz, W.-Y. Leung, H.C. Kang, and P. A. Thiel, Phys. Rev. B **43**, 8834 (1991).

[35]K.-M. Ho and K. P. Bohnen, Phys. Rev. Lett. **59**, 1833 (1987).

[36]*CRC Handbook of Chemistry and Physics,* 67th ed., edited by R. C. Weast, M. J. Astle, and W. H. Beyer (CRC, Boca Raton, FL, 1986–1987), E63.